International Journal of Chemical, Materials and Biomolecular Sciences
ISSN: 2415-6620
Vol:9, No:12, 2015

Rotary Entrainment in Two Phase Stratified Gas-Liquid Layers: An Experimental Study

Yagya Sharma, Basanta K. Rana, Arup K. Das

***Abstract*—**Rotary entrainment is a phenomenon in which the interface of two immiscible fluids are subjected to external flux by means of rotation. Present work reports the experimental study on rotary motion of a horizontal cylinder between the interface of air and water to observe the penetration of gas inside the liquid. Experiments have been performed to establish entrainment of air mass in water alongside the cylindrical surface. The movement of tracer and seeded particles has been tracked to calculate the speed and path of the entrained air inside water. Simplified particle image velocimetry technique has been used to trace the movement of particles/tracers at the moment they are injected inside the entrainment zone and suspended beads have been used to replicate the particle movement with respect to time in order to determine the flow dynamics of the fluid along the cylinder.

Present paper establishes a thorough experimental analysis of the rotary entrainment phenomenon between air and water keeping in interest the extent to which we can intermix the two and also to study its entrainment trajectories.

***Keywords*—**Entrainment, gas-liquid flow, particle image velocimetry, stratified layer mixing.

I. Introduction

THE entrainment process can be related with several day to day life experiences. It is a complex and interesting phenomenon in which deformation of fluids takes place across the interface when subjected to some outside instability/force. This leads to heat and mass transfer between the interfaces of two immiscible fluids. By providing the interface with an external turbulent flux, it is possible to achieve intermixing amongst the fluids which can have unbound advantages. Rotary entrainment is a relatively new domain and exploitation of this phenomenon can lead to chemical reactions which were impossible till now to achieve due to their immiscibility. Rotary entrainment is having plenty of applications in the field of oil and gas industries, chemical and petrochemical industry, pharmaceutical industry, gas-liquid chemical reactors, chemical reaction between immiscible fluids etc. In this study, we deal with entrainment in hydrodynamics field which deals with movement of one fluid into another. Specifically, in the hydrodynamics field, this study tries to exploit the entrainment behaviour between two fluids with the help of a horizontal rotating cylinder between their interfaces. Several research works have been done in this field. One of the earliest works done in this field could be traced back to [1] which presented work on rotating cylinder that is partially submerged in Newtonian fluid. They have used a theoretical approach to calculate the liquid flux picked up by a rotating cylinder, and the variation of the film thickness around the periphery of the cylinder. To predict the film thickness of the film, they assumed that a flat surface is withdrawn obliquely under laminar flow conditions from Newtonian fluids. Further, [2] presented a series of work in this field. They have described a well-rounded set of results stating the dependence of the thickness of the liquid film carried upward by the surface of the cylinder to density ρ, viscosity μ and surface tension σ. Numerical as well as experimental results of this work have been addressed by them for Newtonian fluids. In addition, [3] considered non-Newtonian fluids for their next study in which the horizontal rotating cylinder was partially submerged with a contact angle θ. Reference [4] has developed a film profile equation for a power-law type non-Newtonian fluid. This film profile equation allows computing a unique critical flow regime for each kind of power-law fluid. These fluids are characterised by two rheological constants mainly X and n. Theoretically, they presented an understanding of the balance between viscous, gravitational, and inertial forces, and the basic mechanisms for velocity profile development. In addition, the capillary effect in the internal layer has been accounted for. Up till now, all the methods have been used with only one liquid medium. The same technique could also be used to study viscous flow on the outside surface of a horizontal rotating cylinder for two immiscible fluids. The experimental and theoretical analysis done on this system showed three regions of well-defined behaviour separated by two cataclysmic like transitions. Reference [5] has been able to identify three regions, while rotating a horizontal cylinder between two immiscible fluids.

a) Low removal velocities: A dynamic contact line on the cylindrical surface is observed between the two fluid regions. This velocity regime is observed on the top of the cylinder which was coated with the lighter fluid.
b) Intermediate removal velocities: The moving contact line that is detected in the low removal velocities disappeared and it is sucked up by the movement of the solid surface. The cylindrical surface in this region is coated with both the fluids.
c) Large removal velocities: The lighter fluid layer could not approach the surface of the cylinder and the bottom of the cylinder is the only region which is coated with heavier fluid.

Yagya Sharma, Arup K. Das are with the Department of Mechanical and Industrial Engineering, Indian Institute of Technology Roorkee, Roorkee-247667, India (e-mail: yagya794@gmail.com, akdasfme@iitr.ac.in).

Basanta K. Rana is with the Department of Mechanical Engineering, Indian Institute of Technology Kharagpur, Kharagpur-721302, India (e-mail: basanta.uce@gmail.com).

TABLE I
NOMENCLATURE

Symbol	Quantity	SI Unit
ρ	Density	kg/m^3
θ	Angle of contact	Radian
μ	Viscosity	$N-s/m^2$
σ	Surface Tension	N/m
R	Radius of cylinder	m
X	Rheological constant	$dyne-s^n/cm^2$
n	Rheological constant	Dimensionless constant
υ	Total Velocity Vector of Ink	m/s
α	Contact Angle of Ink	Radian
r(t)	Radial Distance of Ink	m
u	Total Velocity Vector of Bead	m/s
β	Contact Angle of Bead	Radian
$R(t)$	Radial Distance of Bead	m

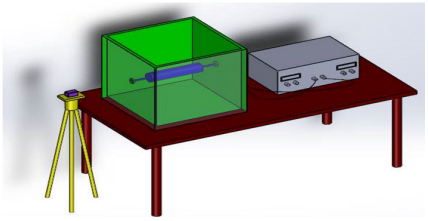

(a)

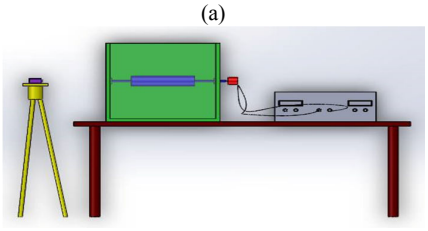

(b)

Fig. 1 Schematic diagram of the experimental setup (a) Highlighting camera and (b) rotor arrangement

Reference [6] has estimated the film thickness around a horizontal rotating cylinder numerically using the volume of fluid (VOF) method to clarify the film-formation process around the rotating cylinder. Parametric studies have been performed to compare the effects of ink properties (viscosity, surface tension) and operational conditions (roller rotational speed, initial immersed angle) on film thickness. Viscosity and rotational speed of the cylinder played a dominant role in determining the thickness of the film.

Until now, all the experimental, numerical and theoretical researches have been done to determine the flow rate and thickness of the film that used to develop due to the rotation of the cylinder. However, up till now entrainment between water-air interface has not been studied experimentally in detail. All the works mentioned before have been used to expound the coating process. Moreover, its utilization in mixing of a two phase fluid has yet not been exploited. Besides, work has still not been done to calculate the height or the distance from the interface till which the entrainment phenomenon is experienced. The film that has been mentioned in the references is basically the entrainment zone which occurs due to drag force applied by the cylinder on the viscous fluids. In this study, an attempt has been made to determine the flow of this entrainment zone using ink dispersion technique, particle image velocimetry, and particle tracking velocimetry. All the above mentioned phenomena has been captured to understand the flow dynamics of fluid-fluid entrainment. Using the results, a theoretical formulation has been performed to understand the process that is undertaken while giving flux to the interface between two fluids with the help of a rotating cylinder.

II. Experimental Detail

A. Design of Experiment

A 50x50x50 cm^3 cubical container made of Perspex sheet is used to build the exterior of the setup. The cubical container is left open at the top, to facilitate easy addition and removal of the fluid. A 30 cm long cylinder of radius 3 cm is mounted on a shaft and fixed along its horizontal axis at the two opposite sides of the container at 25 cm height from the bottom. The shaft extends from one side of the container to provide a mode to mount DC motor on it. To prevent leakage of fluid from the container, washer has been used to air tight the ends of the shaft. DC motor is fixed on the shaft with the help of a screw pin. Motors of different ratings are employed to facilitate different rotational speed to the cylinder. Regulated DC power supply unit gives the reading in the form of voltage and ampere with its output ranging from 0-128V DC and 2.5A MAX. This supply unit is powered by a supply line of 230V AC, 50Hz.With the knob given in the regulated DC supply power unit, proper rating of the motor is achieved. To capture the experimental results, a high speed camera has been used with a frame rate of 500 frames per second. It will be referred to as Camera A in the subsequent texts. In addition, a digital camera of frame rate 25 frames per second with a frame width of 1440 and frame height of 1080 has been used to capture the phenomenon. This will be referred to as Camera B. To facilitate proper lighting two halogen bulbs of 500watt each is engaged on opposite ends of the container. As the setup has been built of Perspex sheet, it is transparent on all sides to facilitate easy observation of the results. However, the right and the back side of the container have been covered with white sheet to pave way for capturing the videos and images of the results. Digital image processing is performed on the captured snaps by the camera. Fig. 1 presents a schematic diagram of the setup.

B. Methodologies

Three procedures have been adopted to consolidate findings on entrainment in the experiment. Initially, the container is half filled with water. A DC motor is fixed to the shaft. The motor is supplied the necessary current by adjusting the DC supply unit to the required ratings of the motor. When the rotor starts rotating the shaft, a distinct entrainment phenomenon is observed between air and water. To elaborate on this observation, several techniques have been used to determine the flow dynamics/trajectories of this entrainment.

One of the methods that have been employed is ***ink dispersion technique***. Ink is specifically injected through an

injection syringe to introduce very precise and trivial volume of ink to the water surface. The flow of the ink has been observed and captured with the help of Camera B.

Further to track the velocity vectors of particles inside the entrainment region, ***Particle image velocimetry (PIV)*** method has been used. In this method, the fluid is seeded with tracer particles. The fluid with entrained particles is observed and the motion of the seeded particles is used to calculate the velocity field of the flow under study. During PIV, the particle concentration is such that it is possible to identify individual particles in an image, but these individual particles cannot be tracked between images. The seeding particles are an inherently critical component of the PIV system. Depending on the fluid under investigation, the particles must be able to match the fluid properties reasonably well. Otherwise, they will not follow the flow satisfactorily enough for the PIV analysis to be considered accurate. Hence, golden glitter particles have been used to determine the region where density of particles is more and in which direction they tend to flow. However, due to the high concentration, the glitter particles which are approximately micron in size have not been able to be tracked. The above proposed method has been monitored by converting the captured video into frames and then observing the particle trajectory. On the other hand, to track individual particles, ***Particle tracking velocimetry*** (***PTV***) method has been used. It is a technique to measure velocity of particles dropped inside the fluid. While PIV technique is an Eulerian method approach, PTV tracks individual particles and follow Lagrangian approach. Golden coloured aluminium balls have been used as the seeding particles to track velocity field in the entrainment region.

III. Experimental Results And Discussions

A. Rotary Entrainment

To observe rotary entrainment phenomenon, 200 rpm, 12V DC motor is fitted to the shaft with its horizontal axis in line with the cylinder's axis. A distinct protuberance of water is visible in the air medium in the direction of rotation of the cylinder. On the other hand, a distinct dip is found on the opposite side of the cylinder along its longitudinal axis. Fig. 2 depicts the cylinder rotating in clockwise direction with a water protrusion in the air medium and a dip in the water due the entrance of air mass.

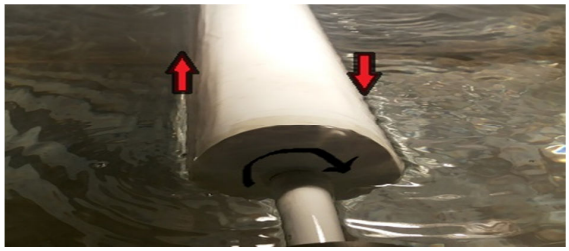

Fig. 2 Rotary Entrainment: Formation of water chute and air chute

Fig. 3 shows the entrance of water in the air medium. This protuberance of a film of fluid in another medium is called chute. In this case, it is the water chute entraining in the air medium.

Fig. 3 Water Chute in Air medium

Fig. 4 depicts the front view of the setup in which a clear indication of water chute is observed entering in the air medium along the direction of rotation of the cylinder.

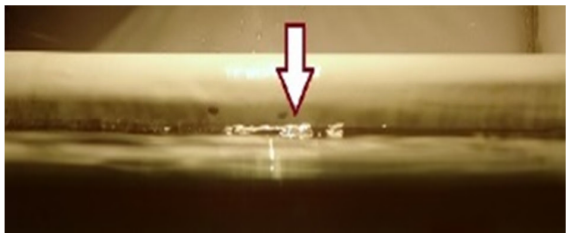

Fig. 4 Front view of the cylinder showing Water Chute in Air medium

B. Ink Dispersion Technique

To determine the flow dynamics of the entrainment, a minuscule drop of ink is injected near the entrainment region. A motor of 200rpm, 12V rating is used to rotate the cylinder. Under the load of water, the shaft rotates at 175rpm. Video is captured with the help of Camera B from the time the water is pigmented with the ink to the time it disperses in the water. The video is then split into frames to observe the ink flow. Ink is injected in the water near the air entrainment region where the formation of air chute takes place. The start point of ink dispersion technique has been shown in Fig. 5.

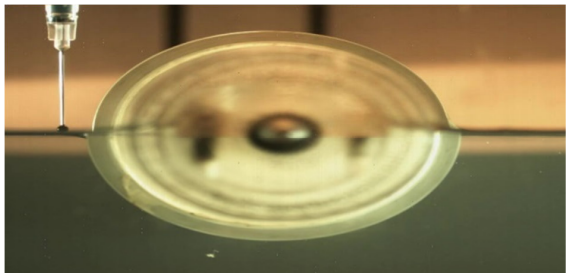

Fig. 5 Start point for ink dispersion technique

It is observed that the ink immediately flows to the region where dip has formed due to the rotation of cylinder. This gives a clear indication of presence of pressure difference at the same level in the container. This leads to the conclusion that an altered region is present near the cylinder that has properties different from rest of the water medium. Further,

the ink follows a specific path covering approximately one fifth of the circumference of the cylinder before getting dispersed. This discrete path followed by the ink could be associated to the fact that the entrainment region of air has its effect inside the water, only till the point where the ink starts to disperse as presented in Figs. 6 (a)-(l).

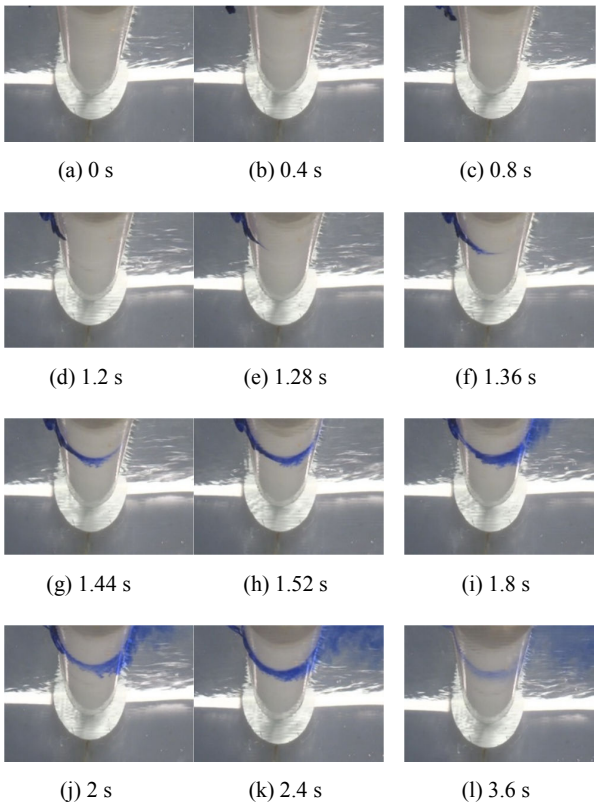

(a) 0 s (b) 0.4 s (c) 0.8 s

(d) 1.2 s (e) 1.28 s (f) 1.36 s

(g) 1.44 s (h) 1.52 s (i) 1.8 s

(j) 2 s (k) 2.4 s (l) 3.6 s

Fig. 6 Ink Dispersion Technique: Flow of pigmentation under influence of entrainment

The images have been discretized and analysed with the help of a scripted code. The tip of the ink is tracked in each picture. Distance and the angle made by the tip of the ink has been measured from the centre of the cylinder. It has been used to calculate the tangential, radial and total velocity using (1), where ***v***is the total velocity vector, ***r(t)*** is the radial distance of ink tip from the centre of the cylinder with time and**α** is the angle made by the ink tip from the centre of the cylinder. An indigenous code has been scripted to analyse the data and determine the velocity vectors for different time stamps.

$$\mathbf{v} = \mathrm{d}\frac{\mathbf{r(t)}}{\mathrm{dt}} = \frac{\mathrm{dR}}{\mathrm{dt}}\boldsymbol{\alpha} + \frac{\mathrm{Rd}\boldsymbol{\alpha}}{\mathrm{dt}} \quad (1)$$

The obtained velocities have been plotted against time. It is observed that the velocity of the tip of the ink increases till the point the entrainment affects the flow dynamics of water around the cylinder. As soon as it ends, the ink starts diffusing in the water. The point at which the ink starts to disperse is the point of maximum velocity and it is the end of air chute. In the initial phase of the graph, we observe an approximately constant velocity. It is the phase where the ink is injected in the water at some distance from the cylinder. Once it reaches the dip, the Velocity-time graph assumes an increasing slope till the point chute reaches its maximum height. After which the graph assumes a decreasing slope and this is the point where ink starts to disperse and effect of entrainment ends. This phenomenon has been represented with the help of a Velocity-time graph in Fig. 7.

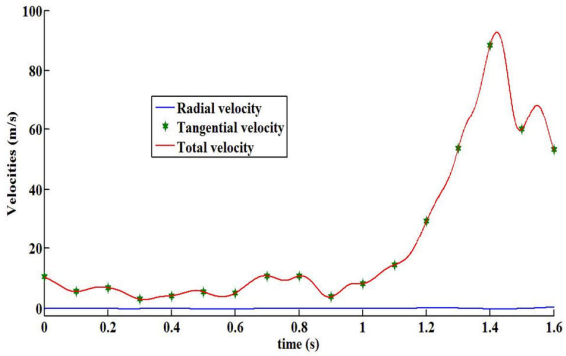

Fig. 7 Total, Tangential, Radial Velocity of Ink tip versus time

C. Particle Image Velocimetry (Piv)

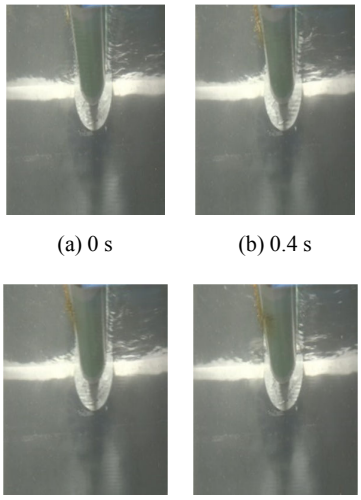

(a) 0 s (b) 0.4 s

(c) 0.8 s (d) 1.2 s

Fig. 8 Particle Image Velocimetry: Flow of seeded particles at different time stamps

A 300 rpm, 12V DC motor has been employed to establish rotary entrainment phenomenon. Golden glitter particles have been dropped from the funnel under the influence of gravity just near the entrainment region. It is witnessed that the glitter particles follow a discrete path just near the cylindrical surface. The particles follow the flow around the cylinder for about one-fifth of the cylinder's circumference. It is observed that in this region, the particles are present in large density and they all move along the cylinder due to the presence of air chute in water. However, once the influence of the air chute diminishes, the particles tend to fall under the influence of

gravity. Hence, it can be stated that entrainment phenomenon makes its presence felt inside water only up to a certain depth. However, it is observed that some of the particles are able to traverse the whole cylindrical surface immersed inside the water medium. This occurrence is due to the pull force associated with the water chute formation in air medium. The flow dynamics of glitter particles is shown in Figs. 8 (a)-(d), which has been captured using Camera A. The depth till which air chute can entrain in the water is dependent on the rpm of the cylinder and the physical properties of the two fluids.

D.Particle Tracking Velocimetry (PTV)

A 300rpm, 12V DC motor has been used to rotate the cylinder. Under the load of water, the rotational speed of the shaft is observed to be 273rpm. Each bead is dropped at a different distance from the air chute. However, it is observed that soon they trace their path towards the entrainment dip and then follow a path alongside the cylinder up to a certain point. This occurrence has been captured with the help of Camera A. The paths followed by the beads have been determined by splitting the videos captured by the camera into frames. Each image has been analysed with the help of a scripted code. Three bead particles are tracked and the distances and angles they make from the centre of the cylinder in the images have been noted with respect to time. Velocity of each bead has been calculated using an in-house code scripted to find out the radial, tangential and total velocity of the bead by using (2), where $\boldsymbol{u}$ is the total velocity vector of the bead, $\boldsymbol{R(t)}$ is the radial distance of the bead from the centre of the cylinder with time and $\boldsymbol{\beta}$ is the angle made by the bead from the centre of the cylinder. The total velocity vector has been plotted against time for the three beads. Fig. 9 displays comparison among the total velocity vectors of the three beads dropped at different distances of 0.5 cm, 0.75 cm and 1 cm away from the cylinder with respect to time, respectively.

$$\mathbf{u} = \mathrm{d}\frac{\mathbf{R(t)}}{\mathrm{dt}} = \frac{\mathrm{dR}}{\mathrm{dt}}\boldsymbol{\beta} + \frac{\mathrm{Rd}\boldsymbol{\beta}}{\mathrm{dt}} \quad (2)$$

After the beads fall on the water surface at 0.5cm, 0.75cm, and 1cm from the entrainment zone, it is observed that the bead nearest to the cylindrical surface has the highest initial velocity and the bead farthest from the cylinder has the lowest initial velocity. The velocity of the beads decreases up till the point they enter the entrainment zone near the surface of the cylinder. However, as soon as they enter the chute, their velocity starts to increase and reaches a maximum value at around 0.6 seconds according to the observed data. These maxima are the end of the area under the effect of air chutes in water. After that, the speed decreases and some of the beads drop under the influence of gravity as the effect of entrainment becomes negligible in that region. Nevertheless, the particles that continue to move along the cylinder again experience an increase in their velocity as they enter the water chute region on the other side of the cylinder. Once the beads reach the apex of the water chute, they reach their maximum velocity before drifting back in the water medium with a decrease in velocity.

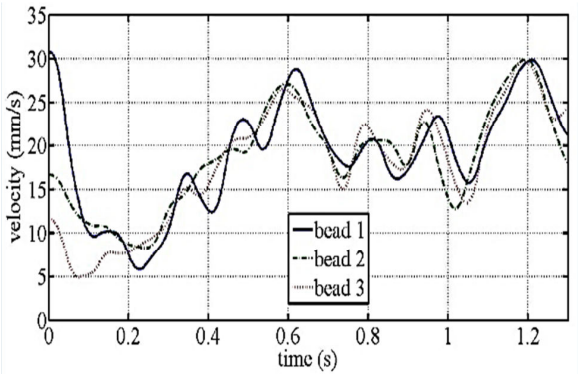

Fig. 9 Total Velocity-time Graph for bead 1 dropped at 0.5cm, bead 2 dropped at 0.75 cm and bead 3 dropped at 1 cm from the cylinder

E. Relation between R.P.M and Entrainment Depth and Radius of Curvature

After arriving at the results related to the flow dynamics of the entrainment region, an indigenous code is scripted to note the changes observed in the entrainment zone with respect to change in the rpm of the rotating cylinder. The setup is run at three different velocities, 165 rpm, 202 rpm, and 243 rpm. It is visually observed, that with increase in velocity of cylinder the penetration of the air-water entrainment zone increases in the nearby region around the cylinder. Hence, two parameters, radius of curvature and maximum depth of entrainment have been taken to represent the physical properties of the entrainment. Videos have been captured using Camera A and has been later analysed frame by frame using an indigenous code to observe the entrainment of air chute inside water at different rpms.

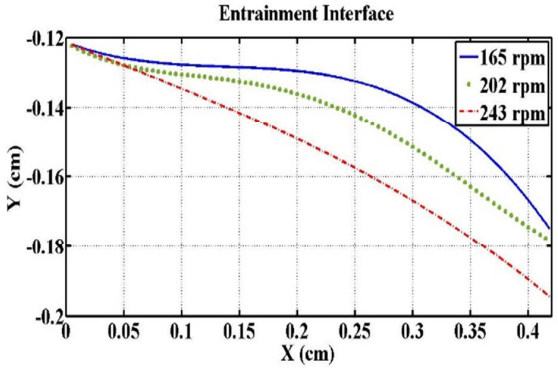

Fig. 10 Interface of entrainment and its depth for different rpm

To quantify the visually observed results, a code is written to capture the pixels of the images near the entrainment region and edge detection technique has been used to obtain the shape of the air chute. For a specific rpm, few images are selected to obtain the time-average curve of the entrainment. From the curve, the depth of the air chutes for different rpms have been obtained. The depth is representative of the fact that the effect of the air chute inside water is only up to this depth. Furthermore, another code has been scripted to find out the radius of curvature of the curve using the points obtained from

previous code. The interface of the entrainment region for different roller speed has been plotted in Fig. 10.

It is observed that with increase in the rotational speed of the cylinder, the radius of curvature as well as the depth of the entrainment increases. That is, the curve starts to become flatter and at the same point the tip of the entrainment zone extends to a deeper region inside water. Table II shows the values of radius of curvature and depth of penetration for respective roller speeds.

TABLE II
PARAMETERS

R.P.M	Radius of Curvature (cm)	Depth of Entrainment (cm)
165	0.8053	0.17484
202	1.3517	0.17901
243	2.0667	0.19788

IV. CONCLUSION

An effort has been made to study the rotary entrainment in water-air interface by a half-submerged cylinder which rotates at different speeds. To estimate the air entrainment zone different techniques have been employed, like ink dispersion technique, Particle Image Velocimetry and Particle Tracking Velocimetry. Variation of total, tangential, and radial velocity of ink tips and golden beads with time have been estimated in detail with different position of impact. The depth of penetration as well as the radius of curvature of air entrainment has been found for different roller rotational speed for half submerged cylinder. It is established that when a cylinder is rotated on the interface of two fluids, an entrainment zone is formed. This entrainment zone is in the form of a dip in the direction of rotation of cylinder. The findings also establish that the chute has maximum velocity at the tip of the entrainment zone. Moreover, it is also established that with an increase in the velocity of the cylinder, the radius of curvature of the chute as well as the depth of entrainment of the zone increases.

ACKNOWLEDGMENT

This paper could not have been possible without the support of Department of Mechanical and Industrial Engineering, Indian Institute of Technology Roorkee and Department of Mechanical Engineering, Indian Institute of Technology Kharagpur, which provided us with the required setup and assistance to accomplish this experiment.

REFERENCES

[1] S. Tharmalingam and W L Wilkinson, "The coating of Newtonian liquids onto a rotating roll," Chemical Engineering Science, Vol. 33,pp. 1481-1487, 20th March 1978.
[2] O. H. Campanella and R. L. Cerro, "Viscous flow on the outside of a horizontal rotating cylinder: The roll coating regime with a single fluid," Chemical Engineering Science, Vol. 39(10), pp. 1443-1449, 1984.
[3] Osvaldo H. Campanella and Jorge L. Galazzo and Ramón L. Cerro, "Viscous flow on the outside of a horizontal rotating cylinder--- II. Dip coating with a Non-Newtonian fluid," Chemical Engineering Science, Vol. 41, No. 11, pp. 2707-2713, 1986.
[4] Cerro R.L. and Scriven L.E., Rapid free surface flows: an integral approach, 1980, Ind. Engng Chem. Fundam. 19, 40.
[5] Osvaldo H. Campanella and Ramón Luis Cerro, "Viscous flow on the outside of a horizontal rotating cylinder---III. Selective coating of two immiscible fluids," Chemical Engineering Science, Vol. 41, No. 11, pp. 2713-2721, 1986.
[6] Seung-Hwan Yu, Kwan-Soo Lee, Se-JinYook, "Film flow around a fast rotating roller." International Journal of Heat and Fluid Flow 30(2009) 796-803.